

Comparison of different approaches for a Multi-Frequency FM Based Passive Bistatic Radar

Pierfrancesco Lombardo, Fabiola Colone, Carlo Bongioanni

Infocom Dept., Univ. of Rome "La Sapienza"

via Eudossiana 18, 00184, Rome, Italy

phone: +39 (0)6 44585472, fax: +39 (0)6 4873300

email: lombardo@infocom.uniroma1.it

ABSTRACT

In this paper we introduce different multi-frequency approaches for improving target detection performance in FM radio based Passive Bistatic Radar (PBR). Specifically, we consider the high diversity of the FM radio signals received over different carrier frequencies spanning the 88-108MHz band since it represents the basis for the request of a multi-frequency operation. The joint exploitation of the waveforms of opportunity received on multiple FM radio channels is shown to yield better performance in terms of detection capability, since it is robust with respect to both the broadcasted radio program content and to the propagation channel conditions. Different multi-frequency integration strategies are proposed and compared to the single-channel operation against the real data collected by a PBR prototype developed and fielded at the Infocom Dept. of the Univ. of Rome "La Sapienza". The availability of live air traffic control registrations allows an overall assessment of the obtained detection results thus showing the performance improvement given by the different multi-frequency approaches.

1.0 INTRODUCTION

In recent years the use of Passive Bistatic Radar (PBR) for surveillance purposes has received renewed interest, e.g. [1]. PBR exploits an existing transmitter as an illuminator of opportunity to perform target detection and localization which results in a number of advantages such as covert operation, low vulnerability, low cost, reduced impact on the environment, etc. The most common signals for PBR in use today are non-cooperative frequency modulated (FM) broadcast radio signals since they offer a good trade off between performance and system development costs, [2]-[3]. A dedicated receiving channel collects the direct signal to be used as reference for matched filtering, which is not under control of the radar designer. Due to the variable and unpredictable characteristics of the transmitted FM waveform, the sidelobes of the ambiguity function for PBR usually have a time-varying structure and a level not much lower than the peak, [4]-[5]. It is therefore likely that target echoes can be masked by the small fraction of the direct signal received by the side/backlobe of the surveillance antenna, by strong clutter/multipath echoes, and even by other targets with higher returns. Thus proper processing techniques should be applied aiming at removing these undesired contributions on the received signal, [6]-[9]. However, the target detection performance is clearly time varying since it is largely dependent on (i) the instantaneous transmitted waveform on the channel under consideration and (ii) on the instantaneous characteristics of the electro-magnetic (e.m.) environment. This time varying behaviour is illustrated in Section 2, since it is the basis for the request of multi-frequency operation. The joint exploitation of the signals of opportunity received on multiple carrier frequencies, corresponding to different FM radio channels, is expected to yield better performance in terms of detection capability, since it is robust with respect to both the content of the broadcasted radio program and to the propagation channel conditions. To this purpose, different multi-frequency (MF) integration strategies are presented in Section 3 together with a statistical

Comparison of different approaches for a Multi-Frequency FM Based PBR

description of the integrated data and the theoretical derivation of the corresponding thresholds to be used after integration by a Constant False Alarm Rate (CFAR) Cell-Averaging (CA) detection scheme. To verify the benefits of the multi-frequency operation and to evaluate the improvement with respect to single channel operation, we have developed an experimental PBR prototype that is able to properly receive the signals broadcasted in the whole FM bandwidth 88÷108 MHz. Section 4 describes the main design features of the developed prototype and the experimental acquisition campaigns that have been carried out in an area with a reasonable density of air traffic. The target detection results obtained over the single channels and after the proposed MF integration strategies are reported and compared to live air traffic control registrations in Sections 5 and 6, respectively. Finally our conclusions are drawn in Section 7.

2.0 INSTANTANEOUS CHARACTERISTICS OF THE FM RADIO SIGNALS

A typical PBR processing scheme is depicted in Figure 1. The signal collected at the reference channel is first used to remove undesired contributions on the surveillance channel. After the cancellation stage, the detection process is based on the evaluation of the Bistatic Range-Velocity Cross-Correlation Function (2D-CCF) between the surveillance signal and the Doppler shifted replicas of the reference signal. A CFAR detection scheme is then applied on the obtained map to automatically detect the potential targets. To show the variability of the detection characteristics with the considered FM radio channel, we need to consider both points suggested in the introduction, respectively addressed in the following sub-sections.

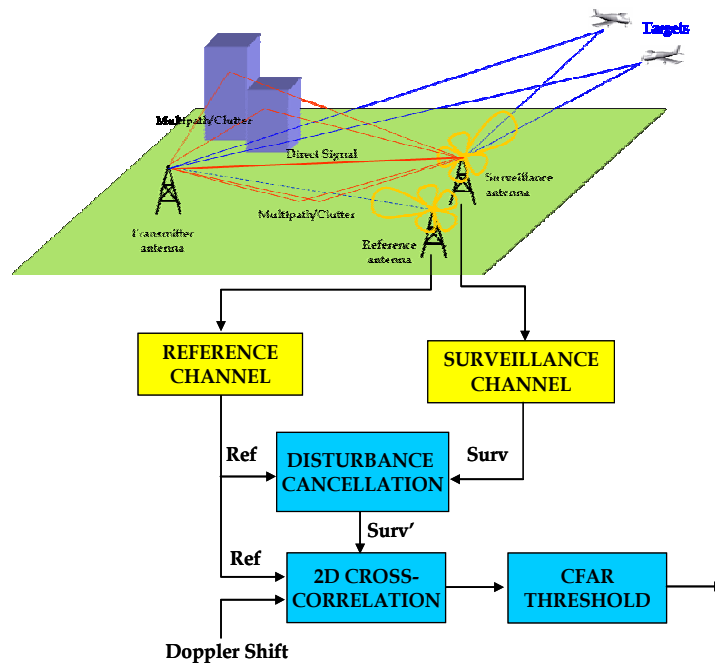


Figure 1: PBR Processing scheme.

2.1 The instantaneous characteristics of the transmitted waveform

The instantaneous transmitted waveform on the considered frequency channel affects the radar range resolution which only depends on the FM signal's bandwidth. Specifically, even if a nominal assigned channel bandwidth of 200 kHz is available for each FM radio channel, a typical FM radio transmission occupies a bandwidth of about 100 kHz thus yielding a range resolution of about 1.5 km. In fact, since the Power Spectral Density (PSD) of a FM signal is proportional to the modulating signal's amplitude distribution, the actual range resolution is strongly affected by the instantaneous transmitted program

content. Both music and voice can reach optimum conditions but usually the music average level is higher than voice, leading to a slightly better range resolution. On the contrary, the presence of long periods of silence or speech pauses in the program content can dramatically degrade the achievable range resolution. As an example, Figure 2(a) reports the spectrograms of different data files of about 1.1 sec length collected at different times for different FM radio channels. The figures clearly show the fast temporal variability of the FM radio signal instantaneous bandwidth and the high diversity of behaviour of the waveforms contemporaneously transmitted at different carriers.

A second characteristic of the self-ambiguity function's analysis concerns the sidelobe level, which is represented in terms of Peak-to-Side Lobe Ratio (PSLR) in Figure 2(b) for 32 different real data tracks ordered on a content basis. Except for the silence, which leads to a periodic ambiguity function, due to the totally ambiguous stereo pilot tone (PSLR = 0 dB), an average value of about -20 dB is obtained for music tracks and slightly higher for voice tracks. These values confirm that the PSLR is a quite important parameter for target detection since it can lead to a significant masking effect of the weak targets. Notice that on each specific FM radio channel the three categories of content are alternatively present, with different durations and timing. Typically the mixing largely depends on the type of radio channel and there is a large variability inside the 88÷108 MHz band.

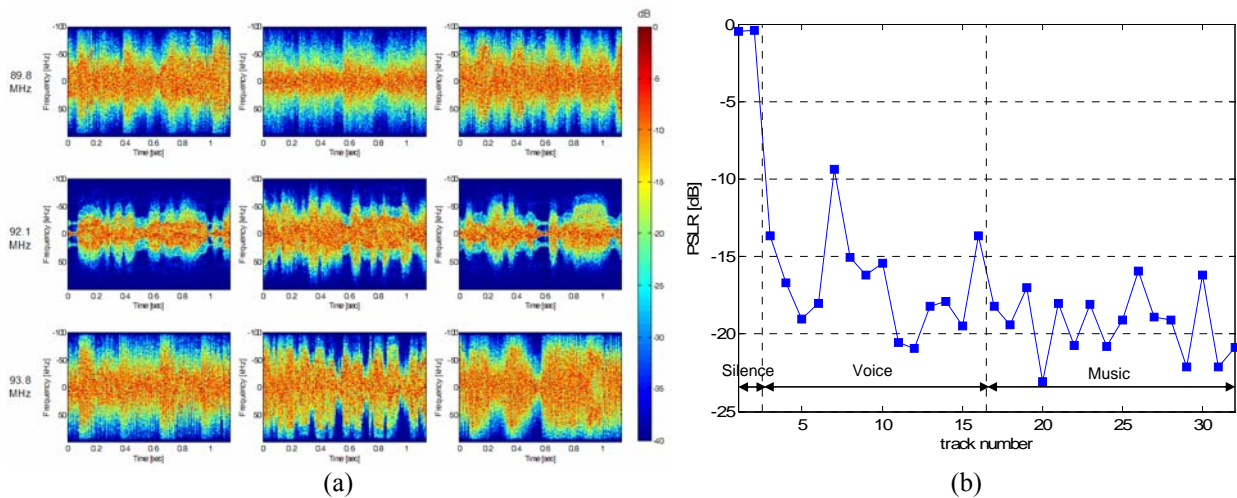


Figure 2: Analysis of the waveform instantaneous characteristics: (a) Spectrograms of the signals collected at different times for different FM radio channels; (b) PSLR of the waveform ambiguity function evaluated over different real data tracks.

2.2 The instantaneous characteristics of the e.m. environment

Among the characteristics of the environment which significantly affect the PBR performance, the multipath returns should be considered. The effect of multipath on both reference channel and surveillance channel is also time varying and can depend both on the specific transmission frequency and on the instantaneous characteristics of the transmitted waveform, [4]-[5]. As an example, Figure 3 shows the modulus and the in-phase component distributions for two registrations of the signals received from the same transmitter at Monte Mario (Rome) at frequencies (a) 90.9 MHz and (b) 92.7 MHz. Following the analysis in [5], it is evident that the distributions in Figure 3(a) are mainly related to thermal noise since they show the typical shape obtained for a constant modulus FM signal in additive Gaussian distributed disturbance. On the contrary, the distributions in Figure 3(b) are dominated by the presence of a strong multipath echo since they appear to be similar to those obtained for the superposition of two delayed replicas of a FM signal and thermal noise. As apparent, even when receiving from the same transmitter, it might be possible to experience different propagation channel conditions on different FM radio channels.

Comparison of different approaches for a Multi-Frequency FM Based PBR

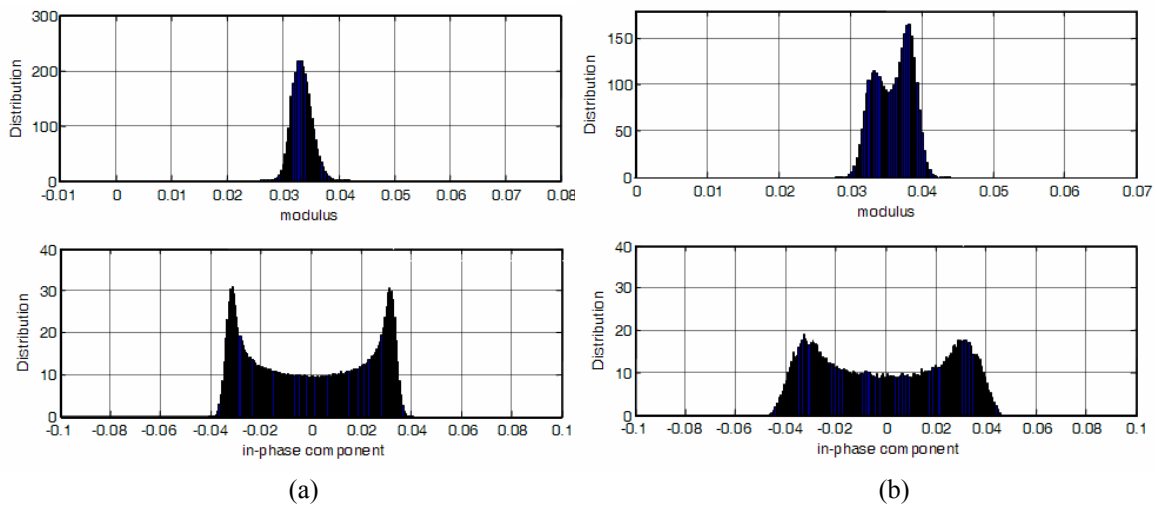


Figure 3: Modulus and in-phase component distributions for two records transmitted by Monte Mario at frequencies (a) 90.9 MHz and (b) 92.7 MHz

Another typical effect related to the PBR e.m. environment is the presence of co- and inter- channel interferences. In fact, due to the high density of FM radio transmissions over the 88 ÷ 108 MHz bandwidth, it is likely that (i) the same frequency is used by different transmitters covering different but neighbouring geographical areas; (ii) a high power transmission is present on a channel adjacent to the selected channel. These undesired signals act as interferences in the selected channel bandwidth thus increasing the system noise floor and consequently reducing the achievable detection performance. As an example, Figure 4 reports the PSD of the data collected at the reference and the surveillance antennas over the 89.7÷92.3 MHz frequency band. The green arrows indicate the carrier frequencies of the FM radio channels broadcasted by the exploited transmitter located in Monte Argentario (Italy).

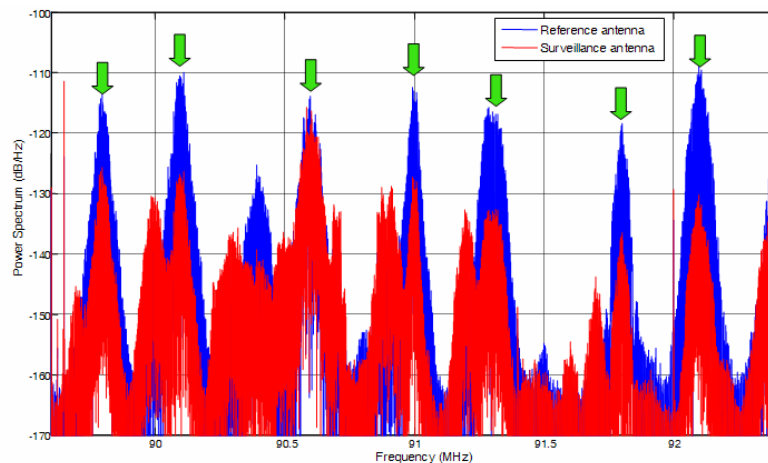


Figure 4: PSD of the data on reference and surveillance antennas over the 89.7÷92.3 MHz band.

As expected, for many of those FM radio channels, the power level measured on the reference antenna is significantly higher than that on the surveillance antenna. Specifically, since the two receiving antennas are identical, almost co-located and steered at 180° apart, and assuming the direct signal coming from the transmitter to be the main contribution to the received power, the ratio of the power levels measured over a single channel on the two antennas should be comparable to the Front-to-Back ratio of the antennas. However, for the channel at 90.6 MHz, the power levels measured on the two receiving antennas are quite comparable: in this case we verified that a co-channel interference affects the surveillance antenna (by

demodulating the corresponding FM signals, different radio programs can be found on the two receiving channels). Moreover notice that the FM radio channels received at the surveillance antenna at 90.1, 91.0, and 91.3 MHz, are highly affected by inter-channel interferences from adjacent frequency channels.

3.0 THE MULTI-FREQUENCY APPROACHES

As apparent from the previous analysis, the availability of N different FM radio channels can collect a huge amount and a large diversity of information. It is then likely that the joint exploitation of the signals of opportunity received on multiple carrier frequencies can improve the detection capability performance, since it is robust with respect to both the content of the broadcasted radio program and to the e.m. environment conditions. Thus the Range-Velocity maps obtained for the different FM radio channels can be incoherently integrated aiming at exploiting the coincidences of detections over different channels while reducing the effects of the single channel waveform/environment characteristics [10].

To this purpose, centralized and decentralized integration strategies can be considered. For a decentralized integration strategy, a threshold is separately applied over the single channels maps and the detection results are subsequently summed up. Using a centralized strategy, different approaches can be considered to build up the final integrated map (as sketched in Figure 5). Three different types of non-coherent integration are obtained by taking respectively the sum, the maximum, and the minimum of the corresponding N pixels' intensity, $z_{n,m}(n=0,\dots,N-1)$, in the single channel maps. Before the different Range-Velocity maps are integrated, a proper normalization should be applied. To this purpose, the actual noise floor can be estimated over a map portion located at high range values, where the target contributions and the effects of the waveforms can be assumed to be negligible. Then this value is used to scale each map in order to yield the same final noise floor.

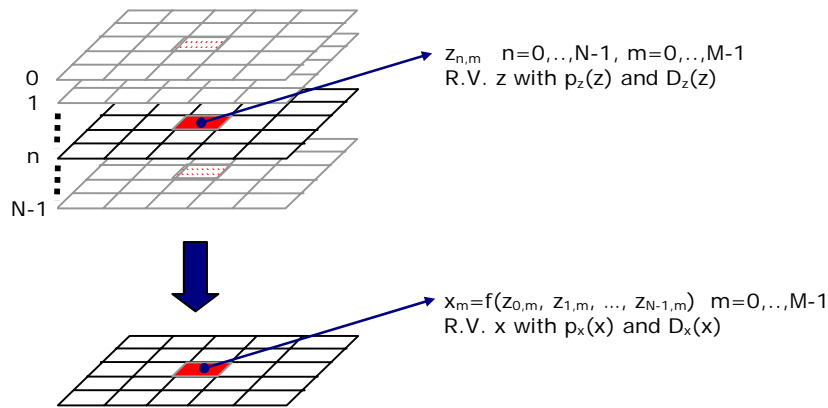


Figure 5: Sketch of the multi frequency approach.

In the hypothesis H_0 (absence of target), we assume the pixels of the original maps to be independent identically distributed (i.i.d.) zero-mean complex Gaussian random variables (r.v.) with variance σ^2 , thus yielding an exponential Probability Density Function (PDF), for the pixels' intensity (square-law detector) on the single channel. In the following the different MF approaches are investigated. Specifically the PDFs of the pixels intensity after integration are evaluated according to different integration strategies and the corresponding CFAR thresholds are derived with reference to a Cell-Averaging (CA) detection scheme.

3.1 Decentralized integration (L/N)

Aiming at reducing the impact of the instantaneous characteristics of the single FM radio channel, a decentralized integration strategy can be considered. Specifically, a detection is declared at a given pixel

Comparison of different approaches for a Multi-Frequency FM Based PBR

when L detections out of N channels are obtained for that pixel over the single-channels maps. Obviously this approach is expected to yield reasonable detection performance improvement when at least L of the N exploited FM radio channels yield a reasonable SNR at the Range-Velocity location of a given target. In this case the resulting P_{fa} depends on the false alarm rate P_{fa}^{SC} obtained over the single channel:

$$P_{fa} = \sum_{i=L}^N \binom{N}{i} P_{fa}^{SC i} (1 - P_{fa}^{SC})^{N-i} \quad (1)$$

Thus, the value of P_{fa}^{SC} sets the CFAR detection threshold to be applied on each channel according to the considered detection scheme; for a CA-CFAR scheme with M secondary data the P_{fa}^{SC} is given by:

$$P_{fa}^{SC} = \left(\frac{M}{G_{SC-CA} + M} \right)^M \quad (2)$$

3.2 Centralized Linear integration (SUM)

Assuming that most of the exploited FM radio channels yield a reasonable SNR at the Range-Velocity location of a given target, the corresponding 2D-CCFs should be incoherently summed aiming at enhancing the resulting SNR on the integrated map and averaging the characteristics of the worse channels with the good ones, thus yielding a limited impact on the detection performance. In this case we have:

$$x_m = \sum_{n=0}^{N-1} z_{n,m} \quad m = 0, \dots, M-1 \quad (3)$$

Thus the PDF of the pixels' intensity under hypothesis H_0 , is given by:

$$p_x(x | H_0) = \frac{1}{(N-1)!} \frac{1}{\sigma^2} \left(\frac{x}{\sigma^2} \right)^{N-1} e^{-\frac{x}{\sigma^2}} \quad x \geq 0 \quad (4)$$

For a CA-CFAR detection scheme, the cell under test (CUT) x_0 is compared with the average pixels' intensity estimated over M secondary data x_1, \dots, x_M . The resulting P_{fa} is given by:

$$P_{fa} = \sum_{n=0}^{N-1} \binom{NM+n-1}{n} \left(\frac{M}{G_{SUM-CA} + M} \right)^{NM+n} \left(\frac{G_{SUM-CA}}{M} \right)^n \quad (5)$$

3.3 Centralized Non-Linear integration (MAX)

Assuming that only one or few of the exploited FM radio channels yield a significant SNR at the Range-Velocity location of a given target, a maximum approach should be used by selecting, for each location, the maximum value among the corresponding single channel maps locations:

$$x_m = \max \{ z_{n,m} \}_{n=0, \dots, N-1} \quad m = 0, \dots, M-1 \quad (6)$$

This approach has the drawback of preserving the sidelobes structures due to the instantaneous characteristics of a single FM channel. The PDF of the pixels' intensity under hypothesis H_0 , is given by:

$$p_x(x | H_0) = \sum_{n=1}^N \binom{N}{n} (-1)^{n+1} \frac{n}{\sigma^2} e^{-n \frac{x}{\sigma^2}} \quad (7)$$

For a CA-CFAR detection scheme, the average pixels' intensity x_{CA} is estimated over M secondary data x_1, \dots, x_M which follow the PDF given in (7). Consequently, the resulting P_{fa} is given by:

$$P_{fa} = \sum_{n=1}^N \binom{N}{n} (-1)^{n+1} \left[\sum_{i=1}^N \binom{N}{i} (-1)^{i+1} \frac{iM}{nG_{MAX-CA} + iM} \right]^M \quad (8)$$

3.4 Centralized Non-Linear integration (MIN)

Aiming at significantly reducing the high peaks in the 2D-CCF due to the instantaneous characteristics of the single FM radio channels, a minimum approach should be implemented by selecting, for each map location, the minimum value among the corresponding single channel maps locations. This approach is expected to yield reasonable detection performance improvement only when all the exploited FM radio channels yield a reasonable SNR at the Range-Velocity location of a given target. In this case we have:

$$x_m = \min\{z_{n,m}\}_{n=0,\dots,N-1} \quad m=0,\dots,M-1 \quad (9)$$

Correspondingly, the pixels' intensity PDF (hypothesis H_0), is still exponential with expected value σ^2/N :

$$p_x(x | H_0) = \frac{N}{\sigma^2} e^{-\frac{Nx}{\sigma^2}} \quad x \geq 0 \quad (10)$$

For a CA-CFAR detection scheme, the average pixels' intensity is estimated by averaging over M exponential r.v.s x_1, \dots, x_M . Thus the resulting r.v. x_{CA} has a Gamma PDF and the P_{fa} is given by:

$$P_{fa} = \left[\frac{M}{G_{MIN-CA} + M} \right]^M \quad (11)$$

4.0 PBR PROTOTYPE DESCRIPTION AND ACQUISITION CAMPAIGNS

Aiming at exploiting the whole $88 \div 108$ MHz frequency band of the FM radio broadcast, a wide-band PBR prototype has been developed and fielded at the INFOCOM Dept. of the University of Rome "La Sapienza", [10], based on a direct radio-frequency (RF) sampling approach. The prototype (Figure 6) is based on a high quality dual channel A/D converter with a wide dynamic range (software selectable) and an input bandwidth of about 100 MHz. By properly selecting the A/D converter sampling frequency by means of an external stable and tunable oscillator, the ADC replicates the input signal in all Nyquist zones. With this approach the baseband replica of the whole $88 \div 108$ MHz frequency bandwidth is achieved (with only a small SNR degradation for the high frequency channels in the bandwidth $[100 \div 108$ MHz]). Two directional FM antennas were used, characterized by a Front to Back ratio greater than 15 dB in order to partially reject the direct signal impinging on the surveillance antenna and a beamwidth of about 60° .

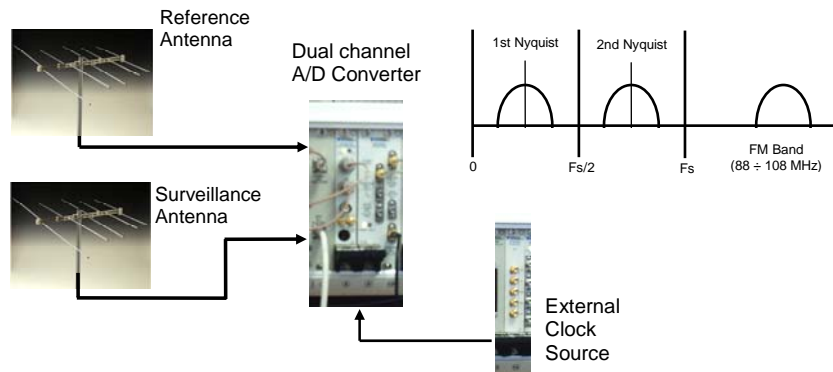


Figure 6: Sketch of the direct RF sampling prototype

Comparison of different approaches for a Multi-Frequency FM Based PBR

Due to the selected values of the sampling frequency, a data flow greater than 220MB/s can be reached thus the main system bottleneck is represented by the PCI bus data transfer rate, 132MByte/s, that does not allow a real-time transfer of the acquired data from the internal A/D memory to the storage disk. To avoid overflow, only short consecutive acquisitions are possible with a single acquisition duration still upper limited by the internal A/D memory size. It should be traded with the temporal separation between consecutive acquisitions which is lower limited by the time required by the data transfer. The acquired and stored data are then off-line elaborated with digital filters to extract the single FM channels of interest.

In the following sections we show the results out of the acquisition campaigns that were carried on May 17th and May 18th 2007 by Riva di Traiano (Civitavecchia) about 70 Km north-east of Rome (Italy), using the prototype described above. The reference antenna was steered toward a transmitter located on Monte Argentario (approximately pointing to north-west), while the surveillance antenna was pointed at about 180° (approximately toward south-east), as illustrated in Figure 7. The transmitter-receiver baseline is of approximately 70 km. A detailed analysis of the data in both temporal and spectral domain suggested the selection of a limited number of FM radio channels. Specifically, four radio broadcast signals were selected transmitted at the following frequencies: 89.8, 92.1, 93.8 and 94.3 MHz. Table 1 reports the details of the selected channels together with the Direct signal-to-Noise Ratios (DNR) measured at the reference and at the surveillance antennas. All these channels correspond to high power transmissions coming from the same transmitter in Monte Argentario while most of them were recognized to have good waveform, co-channel and inter-channel characteristics.

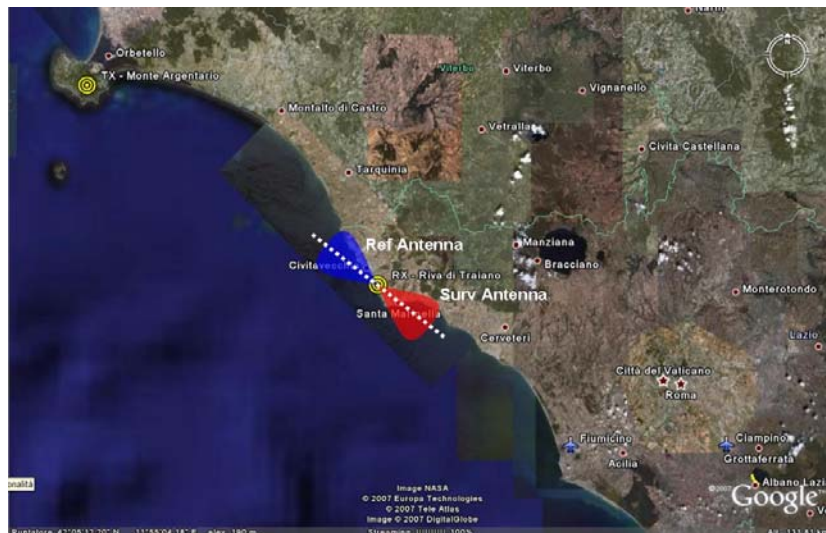


Figure 7: Sketch of the acquisition geometry.

ID	Frequency (MHz)	FM radio broadcast	DNR ref antenna (dB)	DNR tgt antenna (dB)
SFC1	89.8	M20	50.5	38.6
SFC2	93.8	Radio Dim. Suono Roma	52.8	34.7
SFC3	92.1	RAI R.2	56.0	35.6
SFC4	94.3	RAI R.3	57.1	41.8

Table 1: Selected FM radio channels info.

During the considered acquisition campaigns, several sequential data acquisitions were performed; each acquisition is of about 1.1 sec duration, with a temporal spacing of about 23 sec between two consecutive acquisitions. Due to limitations given by the PCI bus data transfer rate and by the internal A/D memory size, the selected time duration represented the best trade-off between the integration time requirement and the temporal spacing between consecutive acquisitions. Data sets acquired with this approach cover a total time duration of about one hour (approximately 150 data files) for each day of the acquisition campaigns.

Correspondingly, live ATC (Air Traffic Control) registrations from Fiumicino International Airport radar have been collected during the acquisition campaigns. These registrations allowed a complete and effective comparison of the results obtained with the single FM radio channels and with the multi-frequency approaches, both in terms of detection probability and false alarm rate (see following sections).

5.0 EXPERIMENTAL RESULTS OVER THE SINGLE FM RADIO CHANNELS

To firstly validate the performance of the single FM radio channel operation, all the available data files have been processed, according to the processing scheme in Figure 1, using the algorithms described in [8]-[9] for direct signal and multipath/clutter cancellation, and a standard bank of matched filters for the cross-correlation. The results have been reported on bistatic Range-Velocity maps to allow a simple and effective comparison of the results achieved on different carrier frequencies.

Figure 8 shows the sequences of the detection results obtained for 3 consecutive data files on the same Range-Velocity map, separately for each of the selected FM radio channels. Also the available ATC registrations have been reported in each figure (grey plots) for comparison. The identified plot sequences are indicated with circles using the continuous green line for complete sequences containing 3 plots and the discontinuous green line for sequences containing only 2 plots.

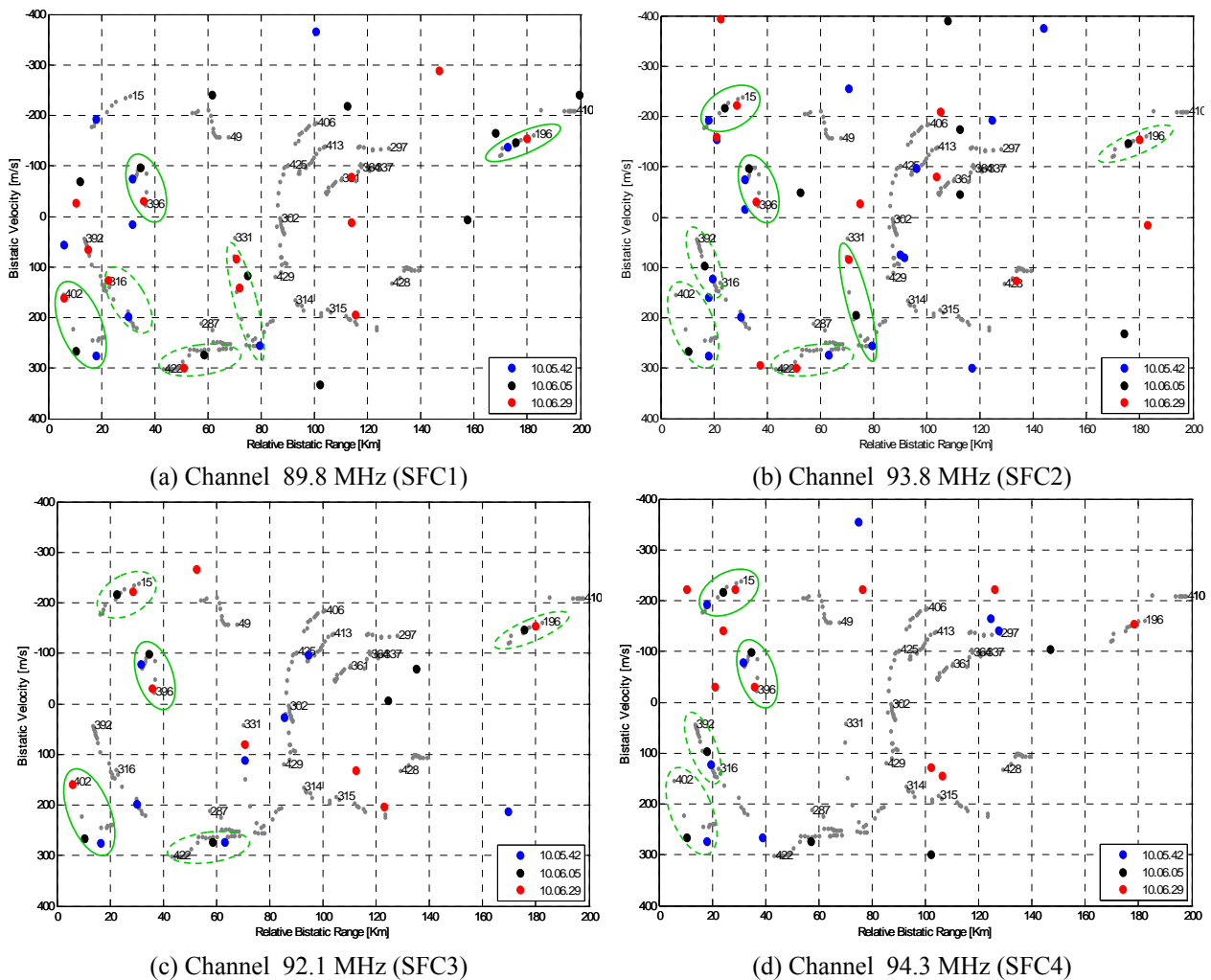


Figure 8: Plot sequences for different FM radio channels for 3 consecutive acquisitions ($P_{fa}=10^{-4}$)

Comparison of different approaches for a Multi-Frequency FM Based PBR

As apparent only on some of the considered channels some quite complete target plot sequences are observed, while on others only few plots are detected. Moreover, not the same target sequences are visible on the different channels. Missed detections are reasonably coincident with general degradation of the characteristics of both the transmitted waveform and the e.m. environment. However the FM radio channels at 89.8 MHz (SFC1) and 93.8 MHz (SFC2) are generally recognized to yield better detection performance due to reduced co- and inter-channel interferences which set the average performance level.

In order to provide an extensive performance evaluation for the single FM channel operation, the detection results obtained with the considered FM channels for all the data sets were compared to the available live air traffic control registrations. An extensive analysis was performed over the 300 recorded data files aiming at estimating the achieved detection probability and the actual false alarm rate. Specifically the performance has been evaluated over proper regions obtained by dividing the considered surveillance volume, contained into the 3 dB surveillance antenna pattern, over the bistatic range and elevation dimensions as depicted in Figure 9. Table 2 reports the results obtained with the different single FM radio channels (SFC1-4) with a CA-CFAR detection scheme for $P_{fa}=10^{-3}$. The table reports the number of true targets observed and detection rate achieved for each region in the grid defined by $\Delta R_x/\Delta E_y$, together with the false alarm rate measured at each range region.

	$\Delta R1$				$\Delta R2$				$\Delta R3$				$\Delta R4$							
	num of targets	SFC1	SFC2	SFC3	SFC4	num of targets	SFC1	SFC2	SFC3	SFC4	num of targets	SFC1	SFC2	SFC3	SFC4	num of targets	SFC1	SFC2	SFC3	SFC4
$\Delta E1$	4	0.00	0.25	0.00	0.00	73	0.03	0.04	0.11	0.07	565	0.10	0.11	0.08	0.07	317	0.05	0.05	0.05	0.04
$\Delta E2$	3	0.67	1.00	1.00	0.33	152	0.28	0.39	0.23	0.20	173	0.23	0.35	0.24	0.13	316	0.12	0.19	0.18	0.09
$\Delta E3$	15	0.87	0.87	0.87	0.53	139	0.45	0.65	0.47	0.35	42	0.29	0.40	0.21	0.21	47	0.15	0.26	0.19	0.13
$\Delta E4$	52	0.75	0.77	0.75	0.69	31	0.68	0.71	0.48	0.42	39	0.26	0.44	0.38	0.10	21	0.05	0.14	0.05	0.10
$\Delta E5$	31	0.58	0.68	0.48	0.45	3	0.33	0.33	0.67	0.33	0	-	-	-	-	0	-	-	-	-
False Alarm Rate		9.6E-4	1.1E-3	9.6E-4	1.0E-3		1.1E-3	1.1E-3	1.1E-3	9.6E-4		1.1E-3	1.1E-3	1.0E-3	8.6E-4		1.1E-3	1.1E-3	1.1E-3	8.8E-4

Table 2: Detection performance for the single frequency channels SFC1-4 (CA-CFAR, $P_{fa}=10^{-3}$)

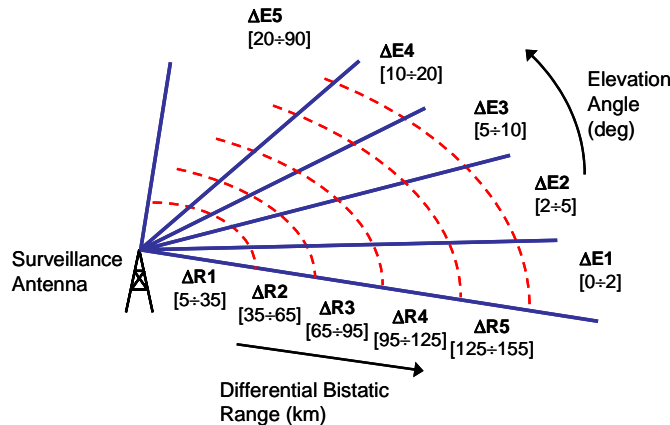


Figure 9: Sketch of the considered regions for the detection performance evaluation

As expected, the detection capability rapidly degrades as the relative bistatic range increases, due to the higher propagation loss. Few detections are obtained among the high number of true targets at low elevation angles, corresponding to the landing aircrafts at Fiumicino airport (see for example the region $\Delta R3/\Delta E1$); this is mainly due to the limited height of the building on which the surveillance antenna is mounted. The obtained False Alarm Rate is largely comparable with the nominal value used to set the threshold. The detection performance highly varies with the considered FM channels at the different detection regions; it is then quite difficult to identify the best performing channel for the whole surveillance volume while we can only observe that, in many cases, different FM radio channels yield complementary or comparable performance.

6.0 EXPERIMENTAL RESULTS OF THE MULTI-FREQUENCY APPROACH

The previous analysis showed that the joint use of N different FM radio channels can collect a large diversity of information, thus potentially improving the detection performance. To this purpose, in the following the MF approaches proposed in Section 3 are applied to the available real data set.

As an example of the detection performance, Figure 10 reports the plot sequences obtained with the different integration strategies after the application of a CA-CFAR detection scheme over the same sequence of 3 acquisitions used in Figure 8 (the decentralized approach operates with $L=2$). For this particular data set of 3 consecutive acquisitions, the best performing integration strategies are the SUM, MAX and DEC approaches which are able to detect many complete plot sequences thus significantly enhancing the performance obtained with the single channel operation (see Figure 8): additional plots are detected for almost all the considered target tracks. This gives a significant advantage especially for targets that result in isolated plots or 2-plot sequences when operating with a single channel, since their tracks are otherwise likely to be lost.

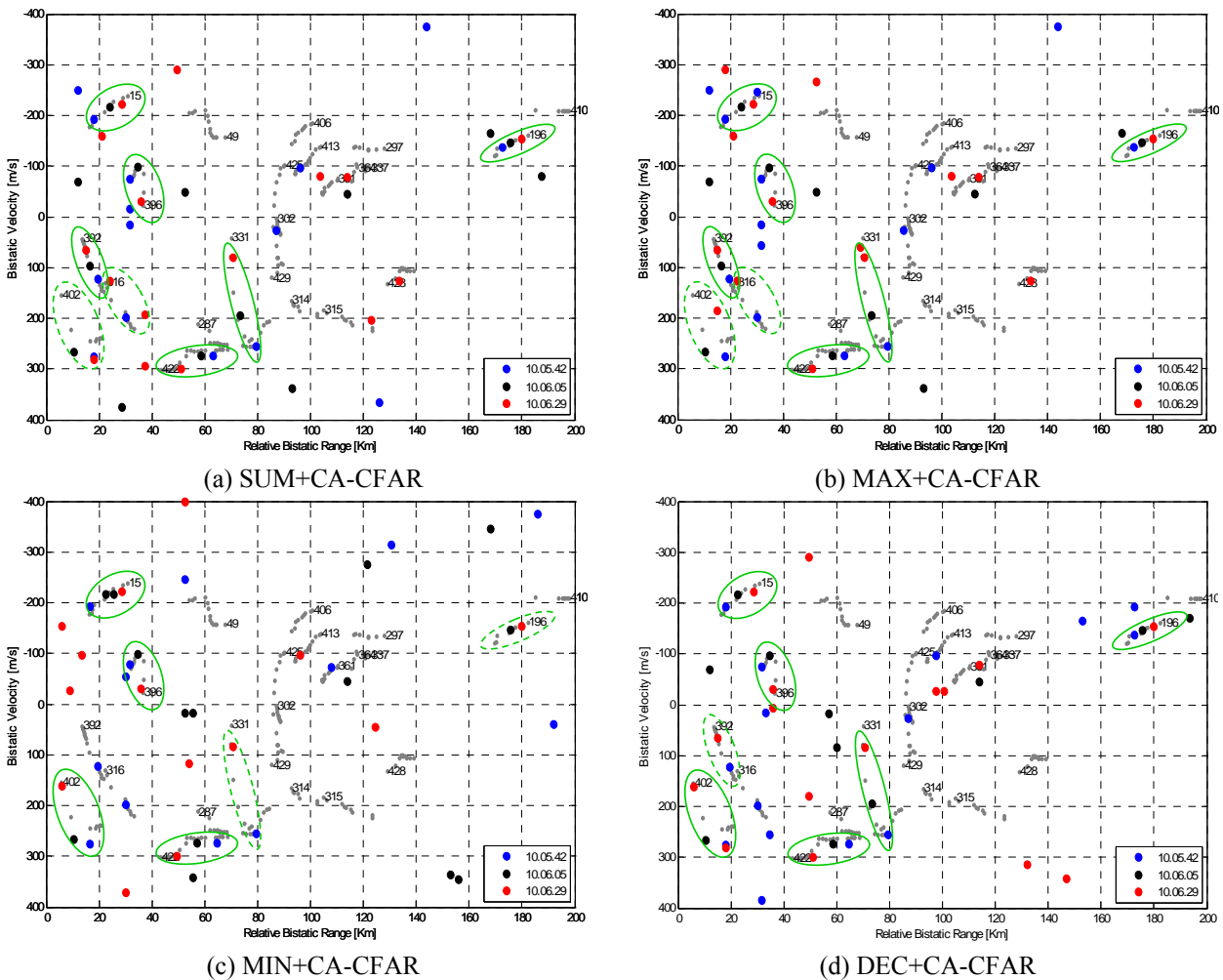


Figure 10: Plot sequences in the Range-Velocity maps for the considered integration strategies obtained using channels at 89.8, 92.1 and 93.8 MHz in the 3 subsequent acquisitions ($P_{fa}=10^{-4}$)

The performance of the MF approaches has been extensively evaluated over the available data as described in Section 5 for the single frequency operation. Specifically, 3 different MF configurations have been considered for all the considered integration strategies:

Comparison of different approaches for a Multi-Frequency FM Based PBR

- MFC2: 2 integrated channels (89.8-93.8 MHz);
- MFC3: 3 integrated channels (89.8-93.8-92.1 MHz);
- MFC4: 4 integrated channels (89.8-93.8-92.1-94.3 MHz).

First of all, aiming at exploiting the detection coincidences achievable over the single frequency channels, the decentralized integration strategy is considered and compared with the single frequency operation in Figure 11 for a CA-CFAR detection scheme. Specifically the figure reports the detection rates achievable with the different single/multi-channel approaches for 3 different bistatic range regions ΔR_1 , ΔR_2 , and ΔR_3 (see Figure 9). For clarity of presentation, these values have been obtained by merging the results obtained for elevation angles in the range 5° - 90° (ΔE_3 , ΔE_4 , and ΔE_5) and discarding the very low elevation angles where the detection performance is limited by the building height (as noticed in the single channel case). The decentralized strategy operates with a “2 out of N ” logic. As apparent, the decentralized integration strategy yields a detection performance improvement with respect to the single frequency operation since, for any given range region, it is possible to find a MF configuration which is able to increase the detection rate with respect to the best performing single channel. Moreover this improvement becomes higher at further bistatic ranges. Notice that the increase of the number of integrated channels does not always yield a performance improvement if the additional channels show poor performance. Thus in the following, the centralized integration strategies are analysed and compared aiming at exploiting the SNR improvement due to the direct (linear or non-linear) integration of the target power at the different channels.

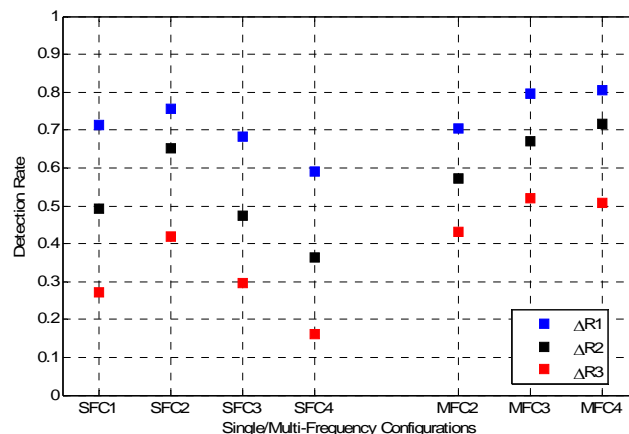


Figure 11: Detection performance comparison among the different single frequency channels (SFC1-4) and the decentralized integration strategies (MFC2-4) for $P_{fa}=10^{-3}$.

Table 3 reports the False Alarm Rates obtained with the different decentralized and centralized integration strategies, distinguishing among the different range regions. As apparent, the obtained False Alarm Rates are largely comparable with the nominal P_{fa} value ($P_{fa}=10^{-3}$), with all the considered integration strategies. Figure 12 shows the comparison of the detection performance obtained with the centralized integration strategies for a CA-CFAR integration scheme. As apparent, for any MF configuration, the achievable detection rate with the MIN approach generally degrades with respect to both the SUM and MAX approaches. Moreover, the best performing MF configuration with the MIN approach always yields worse performance than the worst MF configuration with the SUM approach. In fact, the MIN strategy is able to discard the disturbance residuals and sidelobe structures which appear at a single frequency channel map. However, it retains the minimum SNR for any given target which appears to be a pejorative characteristic when operating with a limited set of frequency channels with highly different SNR.

A global comparison of the proposed integration strategies is shown in Figure 13 for the three considered range regions, respectively. The reported results refer to the best performing integration approaches (DEC, SUM and MAX). Moreover, in each figure the detection rates obtained with the 2 best performing

Comparison of different approaches for a Multi-Frequency FM Based PBR

channels at each range region have been added for comparison. Notice that the detection capability of the considered PBR system is upper limited due to the long baseline between the TX and the RX. Nevertheless, the proposed MF approaches are shown to yield a remarkable performance improvement with respect to the best single-channels for all the considered range regions. Specifically the SUM approach appears to be preferred since it is able to enhance the detection performance with respect to the best performing single channel with all the considered MF configurations. Obviously this performance improvement is paid in terms of computational load since the data from N FM radio channels should be contemporaneously processed. However notice that, in our specific case, further increasing the number of integrated channels does not yield any performance improvement since the additional channels have been recognized to yield poorer characteristics. On the contrary, in some cases, the addition of those channels degrades the detection capability. Obviously, further improvement is expected by adding good-performing channels, when available. In this regard, the capability of automatically selecting the radio frequency channels to be integrated can be of great potential interest since it allows to achieve the desired detection capability without significantly increasing the number of channels and hence the computational load.

	$\Delta R1$			$\Delta R2$			$\Delta R3$		
	MFC2	MFC3	MFC4	MFC2	MFC3	MFC4	MFC2	MFC3	MFC4
DEC	9.7E-4	9.8E-4	1.3E-3	1.1E-3	1.2E-3	1.3E-3	1.0E-3	1.1E-3	1.2E-3
SUM	1.0E-3	1.2E-3	1.9E-3	1.2E-3	1.1E-3	1.4E-3	1.0E-3	1.1E-3	1.2E-3
MAX	1.1E-3	1.3E-3	2.3E-3	1.2E-3	1.2E-3	1.5E-3	1.0E-3	1.1E-3	1.1E-3
MIN	1.1E-3	1.0E-3	1.1E-3	1.2E-3	1.2E-3	1.2E-3	1.1E-3	1.1E-3	1.2E-3

Table 3: False Alarm Rate for the decentralized and centralized integration strategies with different multi-frequency configurations (MFC2-5) ($P_{fa}=10^{-3}$)

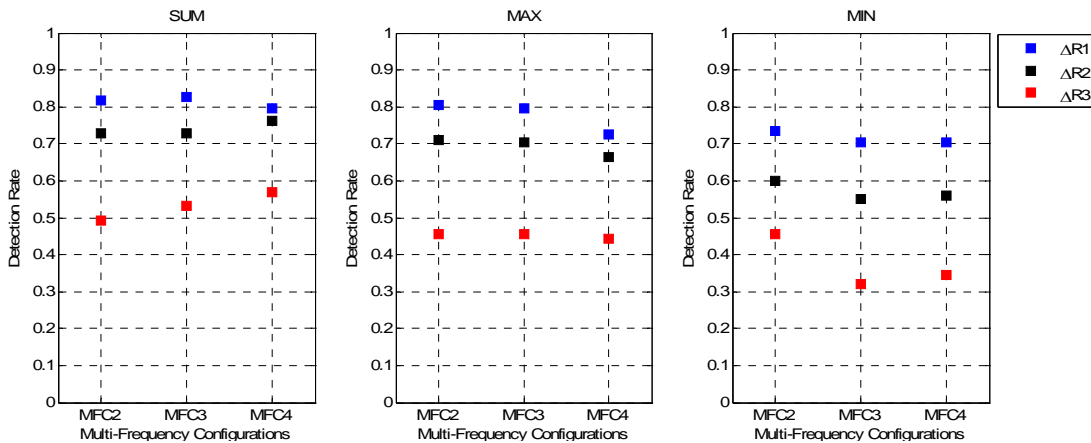


Figure 12: Detection performance comparison among the centralized MF strategies ($P_{fa}=10^{-3}$)

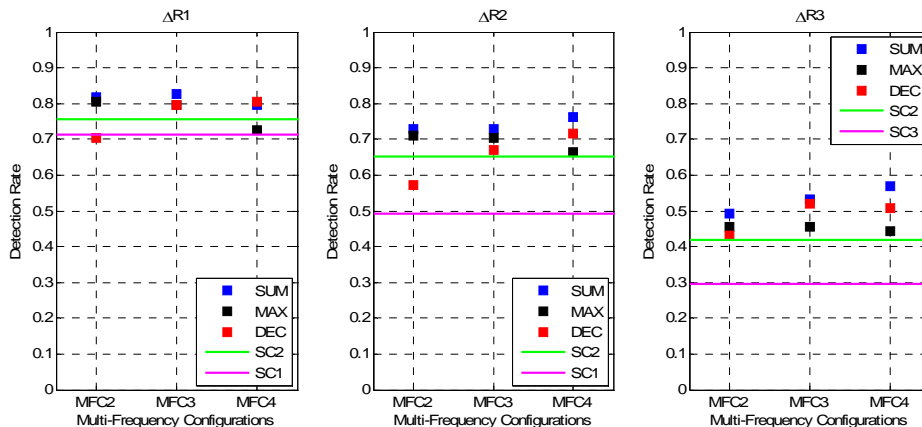


Figure 13: Detection performance comparison among the best MF strategies ($P_{fa}=10^{-3}$).

7.0 CONCLUSIONS

The development of a wide-band PBR prototype has allowed to design and apply different MF approaches that enhance the surveillance capabilities of the PBR, since they make the detection performance robust with respect to both the content of the transmitted radio broadcast channel and the e.m. environment conditions. While better single channel performance would be expected with a narrow band receiving system, the latter would be not robust to the previously mentioned time varying factors (unless considering a system provided with multiple narrow-band channels).

Different decentralized and centralized linear and non-linear integration schemes have been considered in order to jointly exploit the signals of opportunity received on multiple carrier frequencies. Live ATC registrations collected during the acquisition campaigns allowed a complete and effective comparison of the detection results obtained with the single FM channels and the different MF approaches. The proposed MF approaches are shown to yield significantly improved detection performance with respect to the single FM radio channels. Specifically, among the considered integration strategies, the centralized linear scheme (SUM) appears to be preferred in particular when operating with a limited set of frequency channels with different SNR, since it is able to enhance the resulting SNR on the integrated map and to average the degrading characteristics of the worse channels.

References

- [1] Special Issue on Passive Radar Systems – IEE Proceedings on Radar, Sonar and Navigation, June 2005, Vol. 152, Issue 3, pp. 106-223
- [2] P.E. Howland, D. Maksimiuk, G. Reitsma, “FM radio based bistatic radar” IEE Proceedings on Radar, Sonar and Navigation, Volume 152, Issue 3, 3 June 2005 Page(s):107-115.
- [3] Griffiths, H.D.; Baker, C.J., “Passive coherent location radar systems. Part 1: performance prediction” IEE Proc. Radar, Sonar and Navigation, Volume 152, No. 3, June 2005, pp.153-159.
- [4] Baker, C.J.; Griffiths, H.D.; Papoutsis, I., “Passive coherent location radar systems. Part 2: waveform properties”, IEE Proc. Radar, Sonar and Navigation, Volume 152, Issue 3, June 2005, pp.160-168.
- [5] A. Lauri, F. Colone, R. Cardinali, C. Bongioanni, P. Lombardo, “Analysis and emulation of FM radio signals for passive radar”, 2007 IEEE Aerospace Conference, Big Sky (MT), USA, 3-10 March 2007.
- [6] K.S. Kulpa and Z. Czekala, “Masking effect and its removal in PCL radar”, IEE Proc. Radar Sonar Navig., Vol. 152, No. 3, June 2005, pp. 174-178.
- [7] R. Cardinali, F. Colone, C. Ferretti, P. Lombardo, “Comparison of clutter and multipath cancellation techniques for passive radar”, IEEE 2007 Radar Conference, Boston, (MA), USA, March 2007.
- [8] F. Colone, R. Cardinali, P. Lombardo, “Cancellation of clutter and multipath in passive radar using a sequential approach”, IEEE 2006 Radar Conference, Verona (NY), USA, 2006, pp. 393-399.
- [9] F. Colone, D. W. O'Hagan, P. Lombardo, C.J. Baker "A multistage processing algorithm for disturbance removal and target detection in Passive Bistatic Radar" submitted to IEEE Transactions on Aerospace and Electronic Systems, in print.
- [10] C. Bongioanni, F. Colone, S. Bernardini, L. Lelli, A. Stavolo, P. Lombardo, “Passive radar prototypes for multifrequency target detection”, Signal Processing Symposium 2007, Jachranka Village (Poland), 24-26 May 2007.